Graphene Oxide Membranes

DOI: 10.1002/ange.201401061

A Graphene Oxide Membrane with Highly Selective Molecular Separation of Aqueous Organic Solution**

*Kang Huang, Gongping Liu, Yueyun Lou, Ziye Dong, Jie Shen, and Wanqin Jin**

Abstract: *A graphene oxide (GO) membrane is supported on a ceramic hollow fiber prepared by a vacuum suction method. This GO membrane exhibited excellent water permeation for dimethyl carbonate/water mixtures through a pervaporation process. At 25 °C and 2.6 wt % feed water content, the permeate water content reached 95.2 wt % with a high permeation flux (1702 g m^{-2} h^{-1}).*

Graphene oxide (GO), an atomic sheet prepared by oxidative exfoliation of graphite materials, has emerged in recent years as one of the most studied nanomaterials.[1] Its polar oxygenated functional groups, including epoxide, hydroxy, and carboxy groups, give the material many potential uses in various fields, such as optics, gas sensing, composite materials, gas barriers, and nanobiotechnology.[2] Recently, GO-based membranes have been demonstrated to be effective barriers for gas and liquid separation. Several breakthroughs relating to GO-based membranes have been achieved.[3] Geim et al.[3a] found that a GO membrane allowed unimpeded percolation of water while other molecules were blocked. Kim and co-workers[3b] successfully prepared polymer-supported thin GO membranes with high carbon dioxide/nitrogen selectivity. Yu et al.[3c] prepared ultrathin GO membranes (with a thickness approaching 1.8 nm) with high selective hydrogen separation in a facile filtration process. These works demonstrate that GO is a promising membrane material for gas and liquid separation. Herein, we report on a GO membrane for purifying aqueous organic solutions through a pervaporation (PV) process. The GO membrane was prepared on a ceramic hollow fiber by a vacuum suction method, and it achieved efficiently selective water permeation from a water/dimethyl carbonate (DMC) mixture; DMC is an environmentally benign chemical material owing to its hypotoxicity and quick biodegradation.

GO nanosheets are easily stackable because of their single-atom thickness; they have lateral dimensions as high as tens of micrometers and they form stable dispersions in water because they are strongly oxygenated and highly hydrophilic.[1–3] Based on these properties, drop-casting, spin-coating, and filtration are mainly used to fabricate flat GO membranes that are supported on polymeric or anodic aluminum oxide substrates.[3] Compared with planar supports, ceramic hollow fibers exhibit many advantages, such as high-packing density, cost-effectiveness, and chemical and structural stabilities.[4] However, preparing the GO membranes on the surface of ceramic hollow fibers is difficult with these methods owing to the high curvature and elongated shape (Figure 1 a,b). According to the geometric configuration of the ceramic hollow fiber, a vacuum suction method was employed to construct the GO membrane (Supporting Information, Figure S1). GO nanosheets can be easily stacked on the curved surface of the ceramic hollow fiber with pressure as the driving force. This method yields predictably high packing density GO/hollow fiber composite membrane modules. The thickness of the GO membrane can be easily adjusted by controlling the concentration of the GO aqueous suspension or by altering the operation time of the vacuum suction.

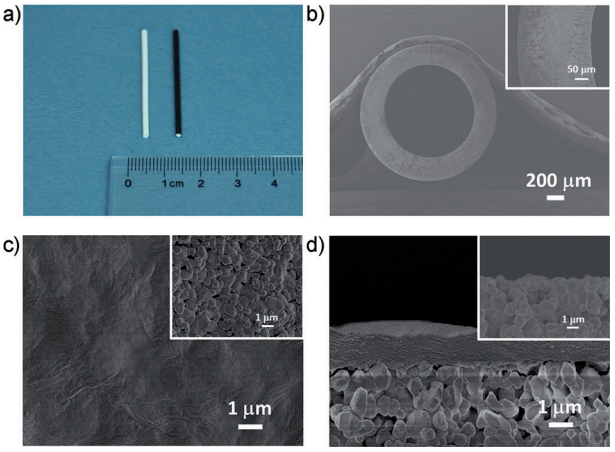

Figure 1. a) Photographs of the blank hollow fiber (white) and the GO membrane (black); SEM images of b) a ceramic hollow fiber (insert: an enlarged cross-section of the ceramic hollow fiber); c) surface and d) cross-section of the blank hollow fiber (inset) and the GO membrane.

Figure 1 a shows an as-prepared GO membrane dried in a vacuum chamber at 40 °C along with a blank ceramic hollow fiber, which reveals a uniform and spindly GO membrane on the ceramic hollow fiber without visible pinholes or cracks under an optical microscope. The color of the GO membrane in Figure 1 a is black, which is different from that of the ceramic hollow fiber (white). It is worth mentioning that the

[*] K. Huang, Dr. G. Liu, Y. Lou, Z. Dong, J. Shen, Prof. W. Jin
State Key Laboratory of Materials-Oriented Chemical Engineering, Nanjing University of Technology
5 Xinmofan Road, Nanjing 210009 (P. R. China)
E-mail: wqjin@njut.edu.cn

[**] This work was financially supported by the Innovative Research Team Program by the Ministry of Education of China (No. IRT13070) and the National Natural Science Foundation of China (No. 21176115 and 21125629).

Supporting information for this article is available on the WWW under http://dx.doi.org/10.1002/anie.201401061.

color of the GO membrane darkens with the increase of thickness of GO membrane from 0.6 to 1.5 μm (Supporting Information, Figure S2). Scanning electron microscopy (SEM) characterization of the surface morphology of the GO membrane is shown in Figure 1c, indicating that the surface is smooth, and no defect was observed except for some nanoscale ripples. Figure 1d shows that the thickness of the GO membrane in Figure 1a is about 1.5 μm with a lamellar structure. The lamellar structure can be clearly observed in an enlarged cross-section SEM image (Supporting Information, Figure S3). According to the atomic force microscopy (AFM) image (Supporting Information, Figure S4), a GO flake is about 1 μm in size with a 1 nm thickness. More detailed X-ray photoelectron spectroscopy (XPS), thermogravimetric analyzer (TGA), FTIR spectroscopy, and X-ray diffraction (XRD) characterizations of the GO powder and the GO membrane were also carried out (Supporting Information, Figures S5–S9). The interfacial adhesion between the GO membrane and the ceramic hollow fiber is an important factor for industrial applications of the GO membrane. Peeling will occur when the interfacial stress surpasses a specific "critical value". The critical load of the GO membrane determined by nanoindentation is 30.62 mN (Supporting Information, Figure S10), confirming that there is a strong binding force between the GO membrane and the ceramic hollow fiber.[5] Furthermore, an optical microscope photo (Supporting Information, Figure S11) also shows that the GO layer did not peel away from the surface of the ceramic hollow fiber after a scratch test, further indicating that the GO membrane bonded well with the ceramic hollow fiber. The strong adhesion force can be attributed to the hydrogen bond between the oxygen-containing functional groups of the GO membrane and the hydroxy group on the surface of the ceramic hollow fiber.

Subsequently, we measured the performance of the 1.5 μm-thick GO membrane for separating DMC/water mixtures, which is a significant step in DMC manufacture. Typically, the product stream from a DMC reactor consists of 50–70% methanol, 30–40% DMC, and 1–3% water. After a basic separation process, the DMC product still contains a small quantity of water.[6] Obviously, using PV for dehydration has many advantages, such as low energy consumption and eco-friendliness, especially when water is a minor impurity in the product that needs to be removed.[7] Herein, three different concentrations of DMC/water mixtures were studied: 1%, 2%, and 2.6% feed water content by weight. To avoid a phase separation in the feed side, the feed water concentration was controlled under 3%.[6b] As shown in Figure 2a, the total permeation flux increases as the operation temperature or the feed water content increases because the driving force is enhanced. Low operation temperatures and high feed water contents are beneficial for obtaining good separation performance (Figure 2b; Supporting Information, Table S1). The activation energy (E_a) of permeation is an important parameter relating to temperature. According to the Arrhenius equation,[8] the E_a of DMC and water was calculated (Supporting Information, Figure S13, Table S2). DMC (23.76 kJ mol^{-1}) has a higher E_a than water (11.12 kJ mol^{-1}) in the PV process with the GO/ceramic hollow fiber composite membrane, meaning that the permeation of DMC through the membrane is more temperature-sensitive than water. After increasing the operation temperature, the permeation flux of DMC increases much more than that of water, resulting in a decrease of the water content permeation and separation factor. The effect of concentration can be explained by the solution–diffusion model.[9] When the feed concentration increases, water can occupy more adsorption sites of GO than DMC because GO is hydrophilic. As a result, the separation performance is improved under higher feed water contents. It is worth pointing out that at 25 °C and 2.6% feed water content, the permeate water concentration is over 95 wt% with a separation factor of 740 and the total permeation flux reaches 1702 g m^{-2} h^{-1}. At 40 °C, this flux will exceed 2100 g m^{-2} h^{-1} with little selectivity degradation. These results are much better than those in previous reports (Supporting Information, Table S3).

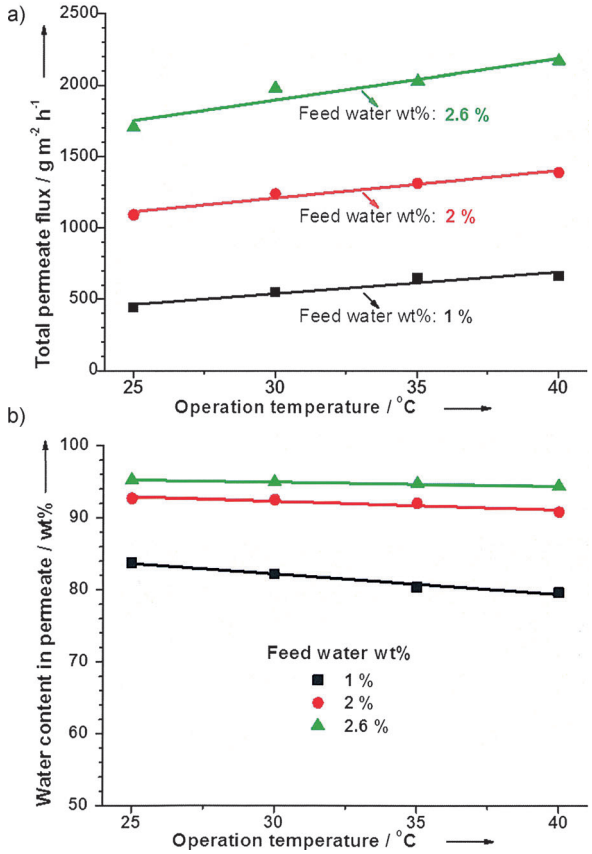

Figure 2. a) Total permeation flux and b) water content in permeate for the separation of DMC/water mixture.

Defects within GO flakes generated by the oxidation reaction and the spacing between GO flakes are the major transport pathway for molecules through the GO membrane. Obviously, as the number of GO layers increases, the function of defects will be weakened because of mutual stacking. Yu et al.[3c] also found that the helium permeance of a 1 μm-thick GO membrane is only 10^{-16} mol m^{-2} s^{-1} Pa^{-1}. Therefore, we speculate that the molecular transport through the 1.5 μm-thick GO/ceramic hollow fiber composite membranes is

mainly dependent on the spacing between GO flakes. To support our inference, we reduced the GO membrane by heating it at 200 °C in a vacuum drying oven and measured the change of water permeance. It was found that the pure water permeation flux of the GO membrane declined from 6254 $g\,m^{-2}\,h^{-1}$ to 83 $g\,m^{-2}\,h^{-1}$ owing to the reduction treatment. The pure water permeation flux decreased approximately two orders of magnitude. This result suggests that the interlayer spacing is the major transport pathway in the PV process because the spacing in the GO layers can be effectively decreased by reduction.[3a,c]

Owing to the existence of groups (such as epoxide, hydroxy, and carboxy groups) at the edges and surface of the GO flakes, the GO interlayer spacing is normally between 0.6 and 1.0 nm, but this depends on the preparation method.[10] This distance is larger than the kinetic diameters of both water (0.265 nm) and DMC[11] (0.47 nm $< d_{DMC} <$ 0.63 nm); namely, water and DMC all can pass through the spacing. However, the PV results show that the water permeation flux is much larger than the DMC permeation flux, although water only accounts for less than 3 % of the feed. It is believed that other separation mechanisms are needed for high-selective molecular separation of DMC/water mixtures using the GO membrane instead of the molecular sieve effect. The separation performance of the PV process is mainly decided by the sorption ability of the membrane surface and the diffusivity through the membrane. A reasonable explanation (Supporting Information, Figure S14) may therefore be that the GO membrane exhibits preferential sorption of water, causing water molecules to gather on the surface of the GO membrane and impede other molecules. On the other hand, the diffusivity of water in the interlayer spacing is much faster than other molecules because of the low-friction flow of water.[3a] Under these effects, high separation performance is achieved. The water permeation by the GO membrane in the PV process follows a preferential sorption–diffusivity mechanism. To support our explanation, we employed a quartz crystal microbalance technique (QCM) to identify the sorption ability of the GO membrane. As shown in Figure 3, upon increasing the experimental time, mass loading of water on the surface of the GO membrane increases rapidly, whereas that of DMC increases very slowly. These results indicate that the GO membrane indeed has a much higher water sorption ability than DMC. Furthermore, we found that the methanol molecules exhibit a moderate sorption ability between those of water and DMC. The corresponding separation performance of the methanol/water mixture (Supporting Information, Figure S16) is lower than that of the DMC/water mixture, further indicating that the sorption ability on the surface of the GO membrane has significant influence on the PV process of the GO membrane. Also, the application of the GO membrane for separating DMC/CH_3OH mixtures exhibits similar results (Supporting Information, Figure S17).

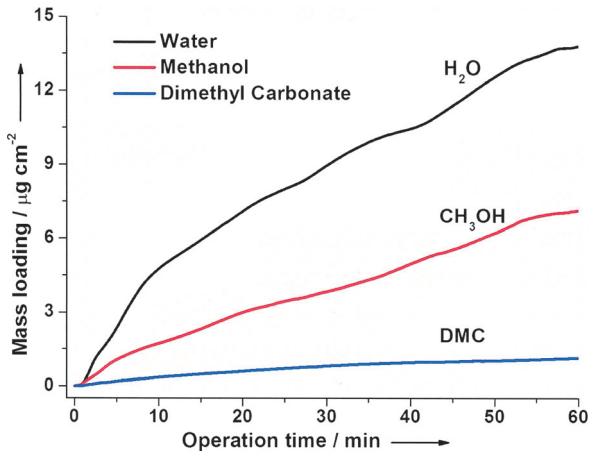

Figure 3. QCM responses of the GO sorption capacity for water (black), methanol (red), and DMC (blue).

In summary, an integrated and continuous GO membrane was successfully prepared on a ceramic hollow fiber substrate by a vacuum suction method, and it exhibited efficiently selective water permeation performance for low toxicity and degradable DMC. The high separation performance of the GO membrane can be attributed to the preferential water sorption ability and fast water diffusivity through the GO layers. Because GO nanosheets can be easily mass-produced by chemical oxidization and ultrasonic exfoliation from inexpensive raw graphite, it is expected that GO membranes are promising candidates for future separation applications, including PV dehydration and gas separation.

Experimental Section

Graphite powder (< 30 μm), $KMnO_4$, 30 % H_2O_2, DMC, and alumina powders were provided by Sinopharm Chemical Reagent Co. Ltd., China. $K_2S_2O_8$ and P_2O_5 were purchased from Jiangsu Yonghua Fine Chemicals Co. Ltd. Concentrated H_2SO_4 and HCl were supplied by Shanghai Shenbo Chemical Co. Ltd. Methanol (CH_3OH, 99.7 %) and deionized water were also employed.

Preparation of GO: GO was prepared by a modified Hummer's method.[12] The following is a typical process. 1) Pretreatment: 3 g graphite powder was added to 12 mL concentrated H_2SO_4 at 80 °C. Then 2.5 g $K_2S_2O_8$ and 2.5 g P_2O_5 were gradually added to the mixture solution for 4 h at the same temperature. After cooling to room temperature, the mixture was diluted with 0.5 L deionized water. Filtering and washing were carried out together to remove excess acid. Then the cake layer was dried until there was no moisture. 2) Oxidization: At 0 °C, 15 g $KMnO_4$ was added extremely slowly to 120 mL concentrated H_2SO_4 which contained the treated graphite powder. After 2 h, 1 L deionized water was gradually added to dilute the mixture while it was in an ice bath. Then 20 mL of 30 % H_2O_2 was added gradually until the mixture turned yellow. The mixture was then washed with large amounts of deionized water and 1 L 10 % HCl solution by centrifugation and dried by freeze drying. Sponge-like GO was obtained.

Preparation of the GO membrane: The GO powder was dissolved into deionized water to make the GO aqueous solution (0.1 $mg\,mL^{-1}$). The resulting GO aqueous solution was treated ultrasonically several times to exfoliate all GO to form GO nanosheets. The membrane preparation process is shown in the Supporting Information, Figure S1. One side of the ceramic hollow fiber was sealed, and the other side was connected to a vacuum pump. GO nanosheets were easily stacked on the surface of the ceramic hollow fiber with pressure driving. After 2 h, a continuous GO/hollow fiber composite membrane was obtained at a pressure of 300–400 Pa. Then the as-prepared GO membrane was dried in a vacuum chamber at 40 °C.

Characterization: The morphologies of the membrane and support were examined by SEM (Quanta-200, Philips FEI). The working parameters were: high voltage (HV) 20–30 kV, work distance (WD) 8–10 mm, and spot 2.0–3.0. The crystal phases of the samples were determined by XRD with Cu Ka radiation (Bruker, model D8 Advance). Diffraction patterns were collected at room temperature in the range of $5° \le 2\theta \le 50°$ with a step width of 0.05° and scan rate of 0.2 s step^{-1}. FTIR spectra were separately recorded in a FTIR spectrophotometer (AVATAR-FT-IR-360, Thermo Nicolet, USA) over the range of 4000–500 cm^{-1}. The dispersion of GO nanosheets was characterized by atomic force microscopy (XE-100 AFM, Park Systems Corp.). The XPS characterization was carried out through an X-ray photoelectron spectrometer (Thermo ESCALAB 250, USA) using monochromatized Al Kα radiation (1486.6 eV). The thermal decomposition behavior of the GO was measured by a TGA (STA449F3, Netzsch) in the temperature range of 30–450 °C with a heating rate of 5 °C min^{-1} in nitrogen atmosphere.

Other experimental characterization techniques, including pervaporation and sorption measurements, as well as scratch testing, are described in detail in the Supporting Information. The fabrication of the ceramic hollow fiber is also described.

Received: January 31, 2014
Revised: March 31, 2014
Published online: May 20, 2014

Keywords: graphene · graphene oxide · membranes · pervaporation · water permeation

[1] a) C. N. R. Rao, A. K. Sood, K. S. Subrahmanyam, A. Govindaraj, *Angew. Chem.* **2009**, *121*, 7890 – 7916; *Angew. Chem. Int. Ed.* **2009**, *48*, 7752 – 7777; b) D. R. Dreyer, S. Park, C. W. Bielawski, R. S. Ruoff, *Chem. Soc. Rev.* **2010**, *39*, 228 – 240; c) J. E. Kim, T. H. Han, S. H. Lee, J. Y. Kim, C. W. Ahn, J. M. Yun, S. O. Kim, *Angew. Chem.* **2011**, *123*, 3099 – 3103; *Angew. Chem. Int. Ed.* **2011**, *50*, 3043 – 3047; d) D. Chen, H. Feng, J. Li, *Chem. Rev.* **2012**, *112*, 6027 – 6053; e) Y. Zhu, D. K. James, J. M. Tour, *Adv. Mater.* **2012**, *24*, 4924 – 4955.

[2] a) G. Eda, G. Fanchini, M. Chhowalla, *Nat. Nanotechnol.* **2008**, *3*, 270 – 274; b) Q. Mei, Z. Zhang, *Angew. Chem.* **2012**, *124*, 5700 – 5704; *Angew. Chem. Int. Ed.* **2012**, *51*, 5602 – 5606; c) J. T. Robinson, F. K. Perkins, E. S. Snow, Z. Wei, P. E. Sheehan, *Nano Lett.* **2008**, *8*, 3137 – 3140; d) H. Kim, Y. Miura, C. W. Macosko, *Chem. Mater.* **2010**, *22*, 3441 – 3450; e) N. Mohanty, V. Berry, *Nano Lett.* **2008**, *8*, 4469 – 4476.

[3] a) R. R. Nair, H. A. Wu, P. N. Jayaram, I. V. Grigorieva, A. K. Geim, *Science* **2012**, *335*, 442 – 444; b) H. W. Kim, H. W. Yoon, S.-M. Yoon, B. M. Yoo, B. K. Ahn, Y. H. Cho, H. J. Shin, H. Yang, U. Paik, S. Kwon, J.-Y. Choi, H. B. Park, *Science* **2013**, *342*, 91 – 95; c) H. Li, Z. Song, X. Zhang, Y. Huang, S. Li, Y. Mao, H. J. Ploehn, Y. Bao, M. Yu, *Science* **2013**, *342*, 95 – 98; d) Y. Han, Z. Xu, C. Gao, *Adv. Funct. Mater.* **2013**, *23*, 3693 – 3700; e) Y.-H. Yang, L. Bolling, M. A. Priolo, J. C. Grunlan, *Adv. Mater.* **2013**, *25*, 503 – 508; f) M. Hu, B. Mi, *Environ. Sci. Technol.* **2013**, *47*, 3715 – 3723; g) H. Huang, Y. Mao, Y. Ying, Y. Liu, L. Sun, X. Peng, *Chem. Commun.* **2013**, *49*, 5963 – 5965; h) P. Sun, M. Zhu, K. Wang, M. Zhong, J. Wei, D. Wu, Z. Xu, H. Zhu, *ACS Nano* **2012**, *7*, 428 – 437.

[4] a) X. Tan, S. Liu, K. Li, *J. Membr. Sci.* **2001**, *188*, 87 – 95; b) Z. Wang, Q. Ge, J. Shao, Y. Yan, *J. Am. Chem. Soc.* **2009**, *131*, 6910 – 6911.

[5] W. Wei, S. Xia, G. Liu, X. Gu, W. Jin, N. Xu, *AIChE J.* **2010**, *56*, 1584 – 1592.

[6] a) W. Won, X. Feng, D. Lawless, *J. Membr. Sci.* **2002**, *209*, 493 – 508; b) W. Won, X. Feng, D. Lawless, *J. Membr. Sci.* **2003**, *31*, 129 – 140.

[7] P. D. Chapman, T. Oliveira, A. G. Livingston, K. Li, *J. Membr. Sci.* **2008**, *318*, 5 – 37.

[8] F. Xianshe, R. Y. M. Huang, *J. Membr. Sci.* **1996**, *118*, 127 – 131.

[9] P. Shao, R. Y. M. Huang, *J. Membr. Sci.* **2007**, *287*, 162 – 179.

[10] a) D. A. Dikin, S. Stankovich, E. J. Zimney, R. D. Piner, G. H. B. Dommett, G. Evmenenko, S. T. Nguyen, R. S. Ruoff, *Nature* **2007**, *448*, 457 – 460; b) Y. Zhu, S. Murali, W. Cai, X. Li, J. W. Suk, J. R. Potts, R. S. Ruoff, *Adv. Mater.* **2010**, *22*, 3906 – 3924.

[11] X. Dong, Y. S. Lin, *Chem. Commun.* **2013**, *49*, 1196 – 1198.

[12] a) Y. Xu, H. Bai, G. Lu, C. Li, G. Shi, *J. Am. Chem. Soc.* **2008**, *130*, 5856 – 5857; b) W. S. Hummers, R. E. Offeman, *J. Am. Chem. Soc.* **1958**, *80*, 1339 – 1339.